



Synthesis, *in silico* Profiling, *in vitro* Anthelmintic and Antibacterial Activities of Novel 6-Bromo-2-Phenyl-3-Substituted Quinazolin-4(3*H*)-ones

BHARGAVI POSINASETTY^{1,2}, KISHORE BANDARAPALLE³, NIHAR PILLARIKUPPAM⁴,
RAJASEKHAR KOMARLA KUMARACHARI^{4,*}, GEETHA BIRUDALA⁵ and ARUGA CHANDRAKALA⁶

¹Senior Clinical Data Manager, PROMETRIKA LLC, Cambridge, MA-02140, U.S.A.

²Government Dental College and Research Institute, Bellary-583104, India

³Department of Pharmaceutics, Sri Padmavathi School of Pharmacy, Tiruchanur, Tirupati-517503, India

⁴Department of Pharmaceutical Chemistry, Sri Padmavathi School of Pharmacy, Tiruchanur, Tirupati-517503, India

⁵Faculty of Pharmacy, Dr. M.G.R. Educational and Research Institute, Velappanchavadi, Chennai-600077, India

⁶Department of Pharmacology, S.V.U. College of Pharmaceutical Sciences, S.V. University, Tirupati-517501, India

*Corresponding author: Fax: +91 877 2237732; E-mail: komarla.research@gmail.com

Received: 26 July 2023;

Accepted: 30 August 2023;

Published online: 31 October 2023;

AJC-21421

In this study, eight novel derivatives of 6-bromo-2-phenyl-3-substituted quinazolin-4(3*H*)-ones were synthesized, which was achieved through the use of bromoanthranilic acid, benzoyl chloride, and different substituted amino synthons. The chemical structures of these compounds through IR spectroscopy, ¹H NMR spectroscopy, and mass spectrometry were successfully characterized. By employing computational tools like PASS, Molinspiration, Osiris, and Swiss ADME, we made predictions about the properties of these molecules. These predictions encompassed factors such as anthelmintic and antibacterial traits, drug-likeness, bioactivity scores, toxicity, and potential molecular targets. Furthermore, we performed *in vitro* assays to evaluate the bioactivities of the synthesized compounds. For anthelmintic effectiveness, the conventional method of assessing paralysis and mortality in earthworms for each compound was followed. The antibacterial efficacy was tested against both Gram-positive and Gram-negative bacterial strains, using the agar cup plate technique. The results of these assays provide valuable insights into the potential of these compounds as agents with anthelmintic and antibacterial properties.

Keywords: Bromo quinazolinones, Toxicity, Biological activity, Anthelmintic activity, Antibacterial activities.

INTRODUCTION

Soil-transmitted helminth (STH) infections rank among the most prevalent infections worldwide, affecting approximately 1.5 billion people, which is about 24% of the global population. These infections primarily impact impoverished and under privileged communities in tropical and subtropical regions, with the highest prevalence found in sub-Saharan Africa, China, South America and Asia [1]. The regions where these parasites are intensively transmitted are home to over 260 million pre-school age children, 654 million school-age children, 108 million adolescent girls and 138.8 million pregnant and lactating women who require treatment and preventive interventions [2,3]. Among these groups, school-age children harbour the highest numbers of intestinal worms, leading to more severe

health consequences, including poor growth, anaemia and cognitive decline. Although current anthelmintic drugs show moderate effectiveness, the risk of reinfection persists, necessitating global efforts to eradicate STH infections [4].

In January 2021, the World Health Organization (WHO) issued a new road map to tackle the burden of disease and death caused by neglected tropical diseases (NTDs). However, the development and spread of antimicrobial resistance by pathogens used to treat NTDs pose a threat to achieving the road map targets. Instances of treatment failure have already been observed in kinetoplastids and the causative organisms of leprosy among bacterial NTDs. Reports have indicated varying degrees of antimicrobial resistance concerning medicines used to treat specific NTDs. Although resistance has been documented in animals for most anthelmintic medicines used in the

NTD programs, there is yet no documented case in humans, but the risk must not be underestimated [5,6].

Anthelmintic treatment plays a crucial role in controlling these worms, but the widespread resistance to most commercially available anthelmintics undermines their effectiveness, necessitating the discovery of new and potent drugs [7,8]. The literature reveals the diverse range of biological actions exhibited by quinazolinone derivatives. Extensive documentation exists regarding the antimicrobial, anthelmintic, antiviral, antifungal, anti-allergic, antitumor and antimycobacterial activities of quinazolinones [6-16]. Recent focus has been on finding novel heterocyclic small molecules with antitubercular, antimicrobial and anthelmintic activities targeting socio-economically important parasites, with the aim of subsequent development [17,18]. In this study, 8 new derivatives of 6-bromo-2-phenyl-3-substituted quinazolin-4(3H)-ones were synthesized, characterized and evaluated their anthelmintic and antibacterial activities. The compounds were synthesized by varying the substitution pattern at the third position of 1,3-benzoxazin-4-one and their *in vitro* anthelmintic and antibacterial activities were assessed. In light of this, the pharmacokinetic and biological properties of the synthesized heterocyclic small molecules using various online web resources were also predicted.

EXPERIMENTAL

All the chemicals used in this study were purchased from reputable suppliers including Sigma-Aldrich Co., USA, Merck, USA, Qualigens Fine Chemicals, India), Loba Chemie Pvt. Ltd., India and Himedia Laboratories Pvt. Ltd., India. The melting points of the synthesized compounds were determined using a digital melting point apparatus with open capillary tubes and the values provided are uncorrected. To assess the purity of the synthesized compounds, TLC was performed on precoated silica gel strips, with a solvent system of hexane: ethyl acetate (2:1). The spots were detected using an ultraviolet chamber.

Infrared spectra (cm^{-1}) were recorded using a SHIMADZU FT-IR 4000 instrument with KBr disks. The CHNO elemental analysis was carried out using the Perkin-Elmer Series II 2400 CHNS/O Elemental Analyzer. Mass spectra were obtained using a JEOL GC mate II GC-Mass spectrometer at 70 eV, employing the direct insertion probe method. Nuclear magnetic resonance (NMR) spectra were acquired using a BRUKER AVIII-500 MHz FT NMR spectrometer. Tetramethylsilane was used as the internal standard and the solvent of choice was DMSO.

Retrosynthetic analysis: It involves the process of breaking down a target molecule's structure into simpler precursor

structures (synthons) along a pathway that eventually leads to readily available starting materials for chemical synthesis. This problem-solving technique allows chemists to work backward from the desired product to identify feasible routes for its synthesis.

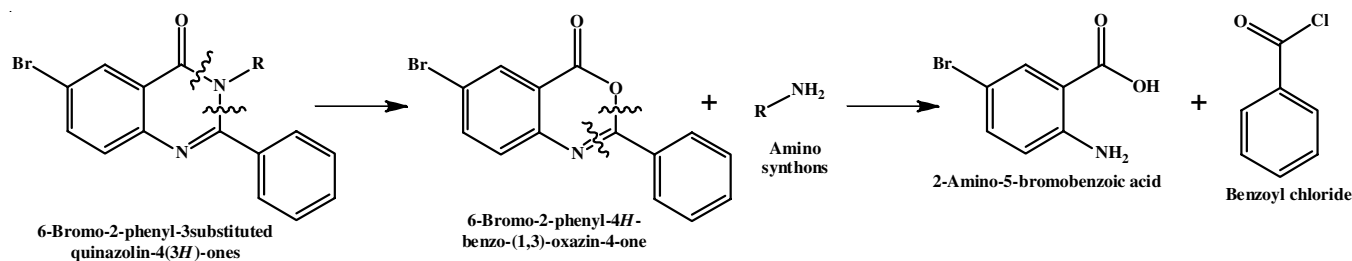
By blocking the two C-N bonds at the third position of the quinazolinone nucleus, we obtained a bromobenzoxazinone compound and a substituted amino fragment as the initial precursors (**Scheme-I**). Further blocking of the C-O and C-N bonds in bromobenzoxazinone led to the formation of bromoanthranilic acid and benzoyl chloride as simple precursors. This process of progressive disconnection and simplification allows us to identify viable starting materials and synthetic pathways for the chemical synthesis of the target molecule.

Synthesis of 6-bromo-2-phenyl-(4H)-benzo[1,3]oxazin-4-one: Dissolved 0.05 mol of bromoanthranilic acid in 30 mL of pyridine and cooled the mixture to 0 °C followed by the addition of 0.04 mol of benzoyl chloride to the reaction mixture and then stirred the mixture for 30 min. Upon treatment of the reaction mixture with 15 mL of 5% NaHCO_3 , a solid product was recrystallized with ethanol to obtain 6-bromo-2-phenyl-(4H)-benzo[1,3]oxazin-4-one. The completion of the reaction was confirmed by performing TLC using hexane:ethyl acetate (2:1) as mobile phase.

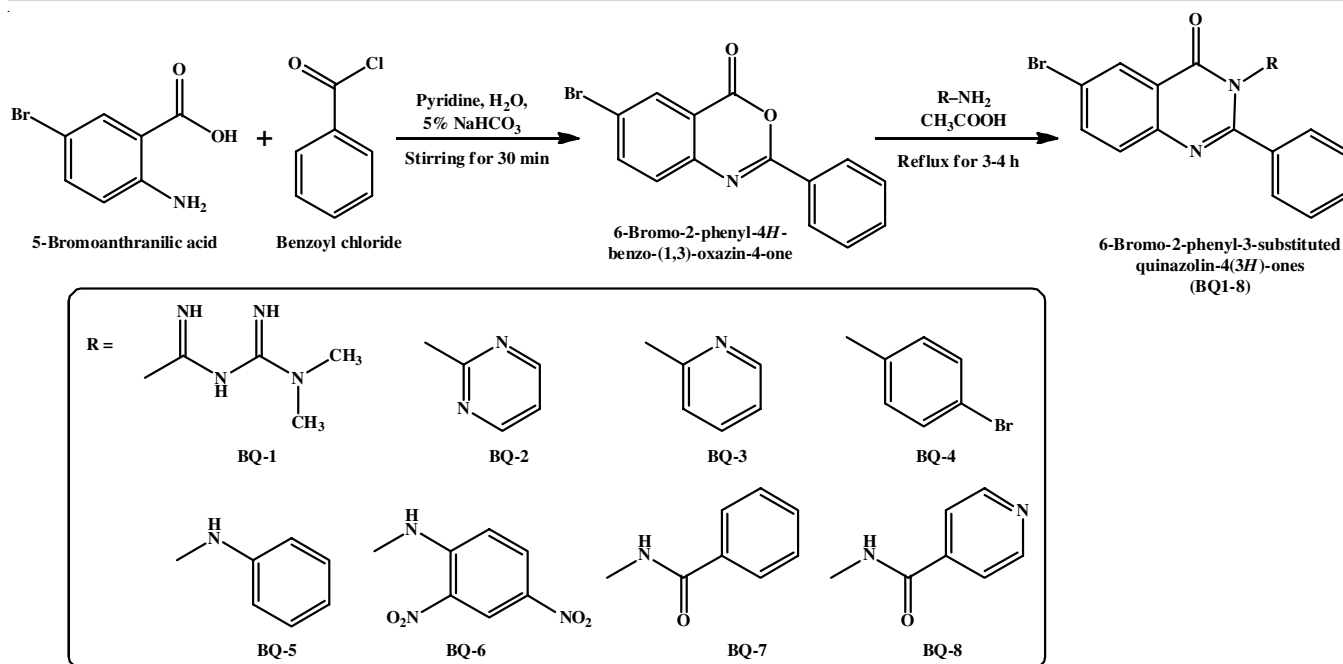
General synthesis of 6-bromo-2-phenyl-3-substituted quinazolin-4(3H)-ones (BQ 1-8): Refluxed 6-bromo-2-phenyl-(4H)-benzo[1,3]oxazin-4-one and the corresponding amino reagent (0.02 mol) in the presence of glacial acetic acid for 3-4 h. Allowed the reaction mixture to cool overnight and then recrystallized the obtained product using ethanol to obtain 6-bromo-2-phenyl-3-substituted quinazolin-4(3H)-ones (**Scheme-II**). The homogeneity and purity of the compounds were confirmed by performing TLC on silica gel G-plates using cyclohexane: ethyl acetate (2:1) as mobile phase and visualizing the spots using a UV chamber [19,20].

Using the same synthetic procedure, compounds **BQ 1-8** were synthesized by employing different amino reagents. The eight amino reagents used are metformin, 2-aminopyrimidine, 2-aminopyridine, 4-bromoaniline, phenylhydrazine, 2,4-dinitrophenylhydrazine, benzohydrazide and isonicotinic acid hydrazide (INH).

6-Bromo-N-(N,N-dimethyl carbamimidoyl)-4-oxo-2-phenyl quinazoline-3(4H)-carboximid amide (BQ1): Yield: 70%, m.p.: 255-260 °C; FT-IR (KBr, ν_{max} , cm^{-1}): 3090 (N-H str.), 1705 (C=O), 1647 (C=N), 528 (C-Br), 1062 (3°N) 1605 ($-\text{CH}_3$); ^1H NMR (DMSO- d_6 , δ ppm): 2.51 (6H, s), 7.39-7.60 (5-ArH), 7.45 (dd), 7.46 (dd), 7.49 (tt), 7.53 (dd, dd), 8.11



Scheme-I: Retrosynthetic analysis of 6-bromo-2-phenyl-3-substituted quinazolin-4(3H)-ones (**BQ1-8**)



Scheme-II: Synthetic scheme of 6-bromo-2-phenyl-3-substituted quinazolin-4(3H)-ones (**BQ1-8**)

(1H, dd), 8.61 (2H, dtd); MS (m/z , %): 413.28 (M^+). Anal. calcd. (found) % for $C_{18}H_{17}N_6OBr$: C, 52.31 (53.14); H, 4.15 (4.08); Br, 19.33 (19.20); N, 20.34 (20.69); O, 3.87 (3.98).

6-Bromo-2-phenyl-3-(pyrimidin-2-yl)quinazolin-4(3H)-one (BQ2): Yield: 82%, m.p.: 203-206 °C; FT-IR (KBr, ν_{max} , cm^{-1}): 1712 (C=O), 1612 (C=N), 528 (C-Br), 1577 (Ar C=C); 1H NMR (DMSO- d_6 , δ ppm): 6.97 (1H, t), 7.48-7.72 (5-ArH), 7.55 (dd), 7.58 (dd), 7.62 (dd), 7.66 (dd), 8.21 (2H, dd), 8.37 (1H, dd), 8.53 (2H, dd); MS (m/z , %): 379.21 (M^+). Anal. calcd. (found) % for $C_{18}H_{11}N_4OBr$: C, 57.01 (56.89); H, 2.92 (2.99); Br, 21.07(21.40); N, 14.77 (14.98); O, 4.22 (4.37).

6-Bromo-2-phenyl-3-(pyridin-2-yl)quinazolin-4(3H)-one (BQ3): Yield: 80%, m.p.: 247-251 °C; FT-IR (KBr, ν_{max} , cm^{-1}): 1721 (C=O), 1662 (C=N), 509 (C-Br), 1620 (Ar C=C); 1H NMR (DMSO- d_6 , δ ppm): 7.19 (1H, dd), 7.36-7.61 (5-ArH), 7.42 (dd), 7.50 (dd), 7.52 (dd), 7.54 (dd), 7.82 (2H, dd), 8.27 (3H, dd), 8.43 (1H, dd); MS (m/z , %): 378.22 (M^+). Anal. calcd. (found) % for $C_{19}H_{12}N_3OBr$: C, 60.34 (60.19); H, 3.20 (3.39); Br, 21.13(21.40); N, 11.12 (11.58); O, 4.23 (4.06).

6-Bromo-3-(4-bromophenyl)-2-phenylquinazolin-4(3H)-one (BQ4): Yield: 80%, m.p.: 222-227 °C; FT-IR (KBr, ν_{max} , cm^{-1}): 1701 (C=O), 1666 (C=N), 547 (C-Br), 1603 (Ar C=C); 1H NMR (DMSO- d_6 , δ ppm): 7.45-7.72 (9-ArH), 7.52 (dd), 7.52 (dd), 7.55 (dd), 7.54 (dd), 7.60 (dd), 7.66 (dd), 8.22-8.41 (3H, dd); MS (m/z , %): 456.13 (M^+). Anal. calcd. (found) % for $C_{20}H_{12}N_2OBr_2$: C, 52.66 (52.31); H, 2.65 (2.89); Br, 35.04 (34.90); N, 6.14 (6.47); O, 3.51 (3.86).

6-Bromo-2-phenyl-3-(phenylamino)quinazolin-4(3H)-one (BQ5): Yield: 68%, m.p.: 185-188 °C; FT-IR (KBr, ν_{max} , cm^{-1}): 3283 (N-H), 1682 (C=O), 1597 (C=N), 543 (C-Br), 1628 (Ar C=C); 1H NMR (DMSO- d_6 , δ ppm): 6.92 (1-ArH, tt), 7.05-7.30 (4-ArH), 7.11 (dd), 7.23 (dd), 7.34-7.64 (5-ArH), 7.40 (dd), 7.51 (dd), 7.54 (dd), 7.57(tt), 8.21-8.36 (3H, dd); MS (m/z , %): 392.24 (M^+). Anal. calcd. (found) % for $C_{20}H_{14}N_3OBr$: C, 61.24

(61.51); H, 3.60 (3.79); Br, 20.37 (20.50); N, 10.71 (10.57); O, 4.08 (4.22).

6-Bromo-3-[(2,4-dinitrophenyl)amino]-2-phenylquinazolin-4(3H)-one (BQ6): Yield: 61%, m.p.: 166-169 °C; FT-IR (KBr, ν_{max} , cm^{-1}): 3217 (N-H), 1635 (C=O), 1581 (C=N), 532 (C-Br), 1602 (Ar C=C), 1493 (C-NO₂); 1H NMR (DMSO- d_6 , δ ppm): 6.97 (1H, dd), 7.17 (1H, dd), 7.48-7.74 (6H), 7.55 (dd) 7.61 (dd), 7.66 (dd), 7.69 (dd), 8.27 (2H, dd); MS (m/z , %): 482.24 (M^+). Anal. calcd. (found) % for $C_{20}H_{12}N_5O_5Br$: C, 49.81 (50.04); H, 2.51 (2.68); Br, 16.57 (16.73); N, 14.52 (14.77); O, 16.59 (16.82).

N-(6-Bromo-4-oxo-2-phenylquinazolin-3(4H)-yl)-benzamide (BQ7): Yield: 72%, m.p.: 216-220 °C; FT-IR (KBr, ν_{max} , cm^{-1}): 1678 (C=O), 1597 (C=N), 558 (C-Br), 1623 (Ar C=C), 1293 (N-H); 1H NMR (DMSO- d_6 , δ ppm): 7.43-7.66 (8H) 7.49 (tt), 7.55 (dd), 7.56 (dd), 7.57 (dd), 7.58 (dd), 7.88 (1H, dd), 8.00 (2H, dd), 8.27 (2H, dd); MS (m/z , %): 420.25 (M^+). Anal. calcd. (found) % for $C_{21}H_{14}N_3O_2Br$: C, 60.02 (60.35); H, 3.36 (3.17); Br, 19.01 (19.18); N, 10.00 (10.15); O, 7.61 (7.43).

N-(6-Bromo-4-oxo-2-phenylquinazolin-3(4H)-yl)pyridine-4-carboxamide (BQ8): Yield: 70%, m.p.: 236-240 °C; FT-IR (KBr, ν_{max} , cm^{-1}): 1663 (C=O), 1591 (C=N), 581 (C-Br), 1608 (Ar C=C), 1323 (N-H); 1H NMR (DMSO- d_6 , δ ppm): 7.48-7.72 (5H), 7.55 (tt), 7.56 (dd), 7.61 (dd), 7.66 (dd), 7.90 (2H, dd), 8.21 (2H, dd), 8.36 (1H, dd), 8.73 (2H, dd); MS (m/z , %): 421.24 (M^+). Anal. calcd. (found) % for $C_{21}H_{13}N_4O_2Br$: C, 57.02 (56.93); H, 3.11 (3.25); Br, 18.97 (18.78); N, 13.30 (13.45); O, 7.60 (7.72).

Prediction of biological activity: The title compounds were subjected to pharmacological activity prediction using the online program PASS. This predictive tool compares the structures of the novel compounds with well-known biologically active substances to identify potential pharmacological

properties, which can later be confirmed through experimental studies.

The advantage of using PASS is that it operates with a vast database of thousands of substances from the training set, providing a more objective estimation of potential biological activities. Moreover, only the structural formula or SMILES of the chemical compound is required to obtain predictions, making it applicable at the earliest stage of investigation [21].

After submitting the structures of all the compounds (**BQ 1-8**) to the PASS online program, various possible mechanisms of action and biological activities were predicted. Among these potential activities, the compounds exhibited a higher probability of being active as anthelmintic and antibacterial agents.

Molinspiration: Molinspiration offers predictions for bioactivity scores related to the crucial drug targets. These targets include G protein-coupled receptor (GPCR) ligands, kinase inhibitors, ion channel modulators, enzymes and nuclear receptors. These bioactivity predictions can be instrumental in drug discovery and development processes, helping the researchers in identifying potential leads for drug candidates that interact with specific drug targets [22].

Osiris property explorer: The Osiris property explorer serves as an essential component within Actelion's in-house substance registration system. It offers the functionality to draw chemical structures and as soon as a structure is valid, it performs real-time calculations of various drug-relevant properties. The prediction results are presented with assigned values and colour codes for easy interpretation.

Properties that pose a high risk of undesired effects, such as mutagenicity, are highlighted in red, drawing attention to potential concerns associated with those properties. On the other hand, properties that are favourable and indicative of drug-like behaviour are displayed in green, signaling promising characteristics for drug development. By incorporating the Osiris property explorer into their system, Actelion can efficiently assess the chemical and pharmacological properties of compounds, helping them make informed decisions during their substance registration process. The drug discovery and development process is accelerated because to the colour coded display, which helps researchers quickly identify molecules with desirable features and potential concerns [23].

Swiss ADME: The prediction tools available on Swiss ADME online platform were employed to ascertain a range of characteristics including physico-chemical properties, lipophilicity, water solubility, pharmacokinetics, druglikeness, molecular target and medicinal chemistry parameters. To estimate the drug-likeness of the compounds, *in silico* absorption, distribution, metabolism, excretion and toxicity (ADMET) predictions were carried out for synthesized compounds **BQ 1-8** were screened using SwissADME software [24].

Anthelmintic activity: The anthelmintic activity was assessed using adult Indian earthworms (*Pheretima posthuma*) due to their anatomical similarity to the intestinal roundworm parasites in humans. For the study, nine groups, each containing six earthworms of approximately equal size, were utilized. Each group was subjected to different treatments: a vehicle

(1% CMC), synthesized compounds and the standard drug albendazole (100, 200, 500, 1000 µg/mL).

Observations were recorded for the time it took for paralysis and death of individual worms. Paralysis was identified when the worms failed to recover even in normal saline. Death was determined when the worms lost their motility and their body colour faded away [25,26].

Antibacterial activity: The synthesized quinazolinones (**BQ 1-8**) were assessed for their antibacterial activity using the agar cup plate method. In this regard, the compounds were tested against both Gram-positive bacteria *Staphylococcus aureus* and *Enterococcus faecium* and Gram-negative bacteria *viz. Pseudomonas aeruginosa* and *Klebsiella pneumoniae* utilizing the MIC method. To establish a comparison, penicillin G and chloramphenicol were used as the reference standards.

Brain heart infusion agar was employed at room temperature for this purpose. The necessary colonies were transferred onto the plates and the turbidity was visually adjusted with broth to match that of 0.5 McFarland turbidity standard after thorough vortexing. To ensure uniform distribution, the entire surface of the agar plate was swabbed thrice, with the plates rotated approximately 60° between each streak.

The inoculated plate was allowed to rest for a minimum of 5 min before the application of drugs. Employing a 5 mm hollow tube, heated and pressed onto the inoculated agar plate, four wells were swiftly created and removed repeated five times across the plate. Following this, 20, 15, 10 and 5 µL of synthesized compounds were introduced into their respective wells on each plate. The plates were then promptly placed in an incubator at 37 °C within 15 min of compound application and incubated for 24 h. The diameter of the inhibition zone was measured to the nearest whole millimeter using a measuring device. Conforming to the MIC procedure, the serial dilution was replicated up to a 10⁻⁹ dilution for each synthesized quinazolinones [27,28].

RESULTS AND DISCUSSION

The 6-bromo-2-phenyl-3-substituted quinazolin-4(3H)-ones (**BQ 1-8**) were successfully synthesized and characterized. All the synthesized compounds were acquired in the form of crystalline needles, each displaying distinct sharp melting points with satisfactory yields. Furthermore, all the synthesized compounds exhibited characteristic peaks in both the FT-IR and NMR spectra. Mass spectra analysis revealed the presence of anticipated molecular ion peak (M⁺) fragments for the synthesized compounds.

In silico profiling: Table-1 presents the biological activity as predicted by the PASS computational program. PASS employs a robust analysis of structure-activity relationships, drawing from an extensive training set of around 60,000 biologically active compounds encompassing approximately 4500 distinct types of biological activities. The calculated probabilities (Pa and Pi) serve to gauge the likelihood of specific compounds exhibiting particular biological activities.

All the compounds synthesized were projected to possess anthelmintic activity, with Pa values registering below 0.5. However, in contrast to this prediction, the experimental evalua-

TABLE-1
PREDICTED BIOLOGICAL ACTIVITY SPECTRUM
OF SYNTHESIZED COMPOUNDS (BQ1-8)

Compound code	Pa	Pi	Activity
BQ1	0.543	0.027	Antibacterial
	0.420	0.026	Vasodilator
	0.213	0.106	Antiprotozoal
BQ2	0.705	0.039	Antiprotozoal
	0.510	0.054	Skeletal muscle relaxant
	0.369	0.045	Antibacterial
BQ3	0.482	0.022	Antibacterial
	0.396	0.032	MAO inhibitor
	0.371	0.077	Antiprotozoal
BQ4	0.530	0.009	Antiprotozoal
	0.460	0.017	Antiviral
	0.367	0.038	Antibacterial
BQ5	0.486	0.014	Antiprotozoal
	0.461	0.030	Antioxidant
	0.421	0.019	Antibacterial
	0.263	0.147	Anthelmintic
	0.263	0.147	Anthelmintic
BQ6	0.356	0.034	Antiprotozoal
	0.344	0.051	Antibacterial
	0.215	0.040	Anthelmintic
BQ7	0.755	0.004	Antituberculosic
	0.727	0.005	Antimycobacterial
	0.233	0.093	Antibacterial
BQ8	0.816	0.003	Antituberculosic
	0.795	0.004	Antimycobacterial
	0.228	0.096	Antibacterial
Albendazole	0.847	0.002	Anthelmintic (nematodes)
	0.828	0.002	Anthelmintic
	0.818	0.003	Antiparasitic
	0.227	0.097	Antibacterial
Pencillin G	0.937	0.001	Penicillin amidase inhibitor
	0.674	0.005	Antibacterial
	0.618	0.012	Antiinfective
	0.475	0.001	Cell wall synthesis inhibitor
	0.460	0.006	Antibiotic
Chloramphenicol	0.901	0.001	Peptidyl transferase inhibitor
	0.723	0.005	Antiparasitic
	0.559	0.007	Antiprotozoal
	0.292	0.040	Anthelmintic

tion demonstrated that all of these compounds exhibited significant anthelmintic activity. This outcome contradicted the initial prediction made by the PASS program.

Molinspiration was employed to predict the bioactivity scores for each of the synthesized compounds as displayed in

Fig. 1. Compounds **BQ1**, **BQ2**, **BQ3** and **BQ8** stood out among the synthesized compounds, demonstrating the significant bioactivity values. These results underscore the potential of these compounds as GPCR ligands, kinase inhibitors and enzyme inhibitors.

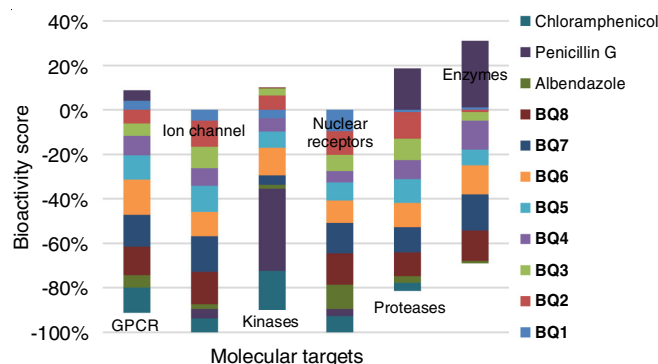


Fig. 1. Calculation of bioactivity scores using molinspiration

Table-2 presents the anticipated toxicological properties and drug score values, as projected by the Osiris property explorer. Promisingly, within the synthesized compounds, it was anticipated that five had a favourable safety profile in relation to toxicity, as evidenced by their accompanying prospective drug score values. Notably, compounds **BQ6**, **BQ8** and **BQ5** were predicted to exhibit toxicity, aligning them with standard drugs employed in *in vitro* studies.

Assessment of drug-likeness was carried out by considering diverse molecular properties and structural features, thereby indicating the potential similarity of these compounds to established drugs. The drug score amalgamates drug-likeness, cLog P, log S, molecular weight and toxicity risks into a single convenient value. This comprehensive metric functions as a tool for evaluating the overall potential of a compound to fulfill the criteria for drug qualification. With the exception of compound **BQ6**, all other synthesized compounds achieved satisfactory scores in terms of their suitability for drug qualification.

Selected physico-chemical, pharmacokinetic and medicinal chemistry properties were predicted using Swiss ADMET and are summarized in Table-3. All the synthesized compounds adhered to Lipinski's rule, a crucial criterion for drug-likeness. Parameters such as molecular weight, Clog P (lipophilicity)

TABLE-2
PREDICTIVE TOXICITY PROPERTIES USING OSIRIS MOLECULAR PROPERTY EXPLORER

Compound code	Drug likeness	Drug score	Mutagenicity	Tumorigenicity	Irritant	Reproductive toxicity
BQ1	4.44	0.84	No	No	No	No
BQ2	2.14	0.78	No	No	No	No
BQ3	2.64	0.76	No	No	No	No
BQ4	1.29	0.51	No	No	No	No
BQ5	0.82	0.35	No	Yes	No	No
BQ6	-8.82	0.05	Yes	Yes	Yes	Yes
BQ7	2.70	0.77	No	No	No	No
BQ8	3.31	0.29	No	Yes	No	Yes
Albendazole	-2.08	0.31	No	No	No	Yes
Penicillin G	11.28	0.33	Yes	Yes	No	No
Chloramphenicol	-4.61	0.06	Yes	Yes	Yes	Yes

TABLE-3
PREDICTION OF PHARMACOKINETIC AND MEDICINAL CHEMISTRY PROPERTIES USING SWISS ADME

Compound code	GIA ^a	BBBP ^b	P-gpS ^c	log Kp (cm/s) ^d	BAS ^e	PAINS Alert	SA ^f
BQ1	High	No	No	-6.44	0.55	0	3.25
BQ2	High	Yes	No	-6.20	0.55	0	2.74
BQ3	High	Yes	No	-5.73	0.55	0	2.88
BQ4	High	Yes	No	-5.20	0.55	0	2.63
BQ5	High	Yes	No	-5.07	0.55	0	3.17
BQ6	Low	No	No	-5.47	0.55	0	3.54
BQ7	High	Yes	No	-5.75	0.55	0	3.09
BQ8	High	Yes	No	-6.51	0.55	0	3.10
Albendazole	High	No	No	-5.92	0.55	0	2.41
Penicillin G	High	No	No	-7.04	0.56	0	3.98
Chloramphenicol	High	No	No	-7.46	0.55	0	2.66

^aGastrointestinal absorption, ^bBlood brain barrier permeant, ^cP-gp substrate, ^dSkin permeant, ^eBioavailability score and ^fSynthetic accessibility

and the counts of hydrogen bond donors (HBD) and acceptors (HBA) were well within the specified limits. The number of rotatable bonds, a fundamental topological descriptor, indicated that the synthesized compounds possess flexibility, a quality that bodes well for their potential oral bioavailability. This descriptor is rooted in any single non-ring bond connected to a non-terminal heavy atom.

Furthermore, the topological polar surface area (TPSA) is a valuable predictor for drug transport properties, encompassing the sum of surfaces attributed to polar atoms (typically oxygen, nitrogen and their attached hydrogens) within a molecule. This parameter has demonstrated strong correlations with vital aspects like human intestinal absorption, permeability across Caco-2 monolayers and penetration of the blood-brain barrier.

Table-3 shows that with the exception of compound **BQ6**, all the synthesized compounds have shown significant levels of passive gastrointestinal absorption in humans. Moreover, compounds **BQ1** and **BQ6** do not possess a blood-brain barrier (BBB) permeant prediction. It is interesting to observe that none of the synthesized compounds exhibit skin permeability or pan assay interference structural alerts (PAINS) as predicted. Furthermore, it was determined that none of the compounds in the study were anticipated to function as substrates of P-Glycoprotein. This interpretation was drawn based on the utilization of a support vector machine (SVM) model, which was developed using a training set consisting of 1033 molecules. The accuracy of the model was then assessed by validating it with a separate test set of 415 molecules.

Based on the analysis using 1024 fragmental contributions (FP2), all the compounds **BQ 1-8** were predicted to be easily synthesized (2.63-3.54), with a scale ranging from 1 (very easy) to 10 (very difficult). This prediction takes into account size and complexity penalties and the model was trained on a dataset of 12,782,590 molecules and validated with 40 external molecules, resulting in a strong correlation ($r^2 = 0.94$). Importantly, this prediction aligns well with the percentage yields observed for the synthesized compounds.

Molecular target predictions carry significant relevance and utility in the domain of drug design and discovery. As depicted in Fig. 2, the highest probable targets for the synthesized bromoquinazolinones are revealed. The enzymes, kinases and G protein

coupled receptors emerged as principal targets for the synthesized compounds. This study could serve as a tool to grasp the molecular mechanisms that underlie distinct phenotypes or bioactivities, offering insights into potential side effects and prognosticating off-target interactions.

Anthelmintic activity: In the assessment for anthelmintic activity, all the synthesized bromoquinazolinones underwent testing on *Pheretema posthuma* at varying concentrations (100, 200, 500 and 1000 $\mu\text{g/mL}$), with albendazole employed as the standard drug. Remarkably, all the synthesized compounds (**BQ1-8**) displayed anthelmintic activity as indicated in Table-4. Of particular interest, compound **BQ7** exhibited the highest potency, followed by **BQ5**, **BQ8**, **BQ1**, **BQ6**, **BQ2**, **BQ4** and finally **BQ3**, in descending order of effectiveness.

As compound **BQ7** contains a polar benzamido group at the 3rd position of bromoquinazolinone ring, demonstrated promising activity. A similar trend was observed with compound **BQ8**. Similarly, in case of compounds **BQ5** and **BQ6**, the presence of an aniline or a polar substituted aniline group likely to contribute to an enhancement in anthelmintic activity. Moreover, it is found that a reduction in the distance between the nitrogen at the 3rd position of the quinazolinone ring and its substituent corresponded with a decrease in anthelmintic activity. This suggests a correlation between the proximity of the substituent and the observed decrease in anthelmintic potency. Indeed, the presence or absence of hydrogen bond contributors between the 3rd position and its substitution played a significant role in influencing anthelmintic activity.

The ability of molecules to form hydrogen bonds, particularly between the polar functional groups, can impact their interactions with biological targets and their overall effectiveness as anthelmintic agents. This highlights the intricate relationship between molecular structure and activity in the context of anthelmintic evaluation. The study suggests the necessity for the synthesis of additional compounds featuring diverse substituents at the 3rd position of the bromoquinazolinone ring. Such endeavours hold the potential to yield more potent anthelmintic agents.

Antibacterial activity: Furthermore, the antibacterial activity of all synthesized quinazolinones was assessed through screening using the agar cup plate method. Specifically, for Gram-positive bacteria such as *Staphylococcus aureus* and

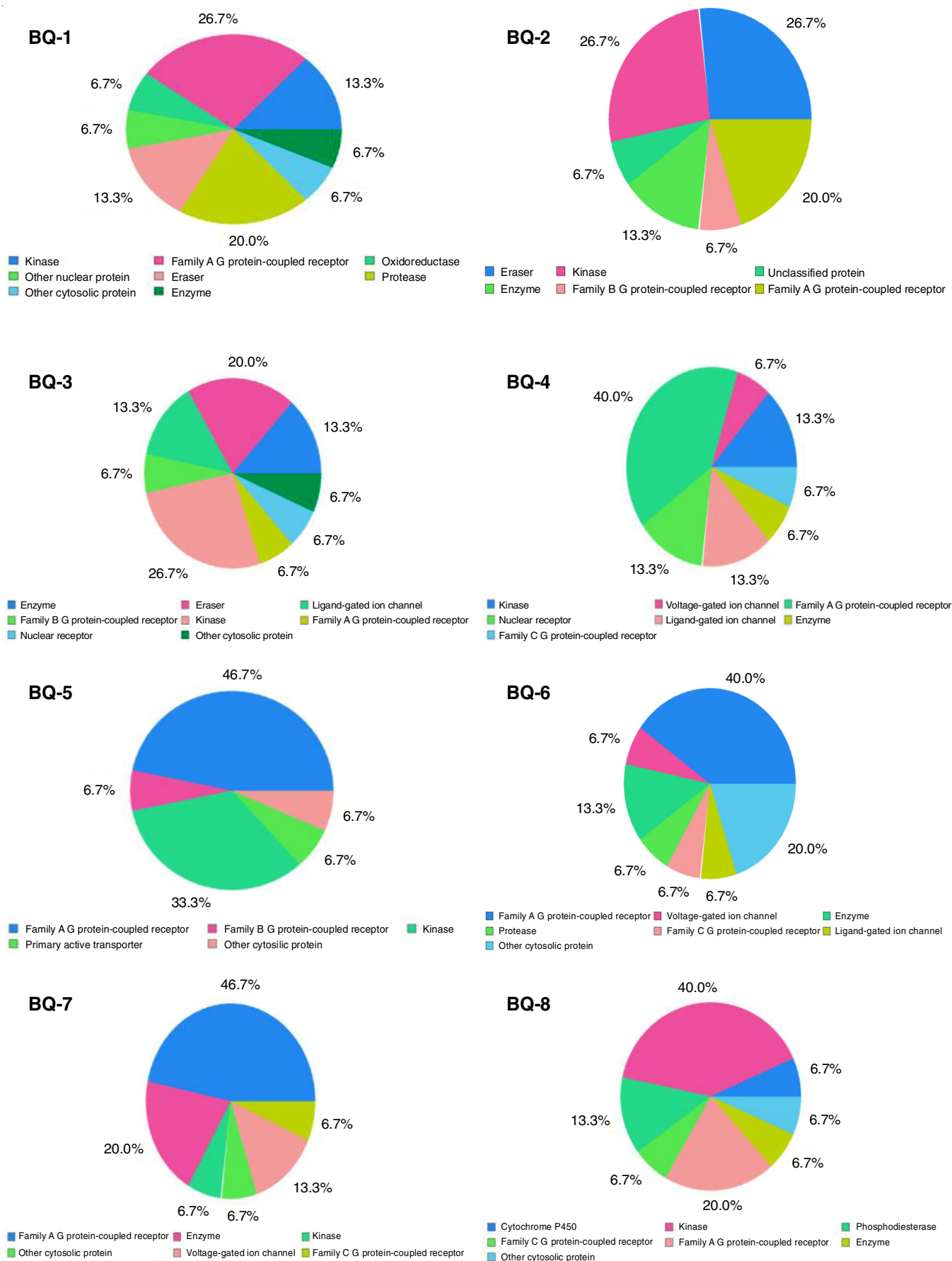


Fig. 2. Top molecular target classes of 6-bromo-2-phenyl-3-substituted quinazolin-4(3H)-ones (BQ1-8)

TABLE-4
ANTHELMINTIC ACTIVITY OF THE SYNTHESIZED COMPOUNDS **BQ1-8**

Concentration (µg/mL)	Onset of paralysis (min)	Onset of death (min)	Onset of paralysis (min)	Onset of death (min)	Onset of paralysis (min)	Onset of death (min)
	BQ-1		BQ-2		BQ-3	
100	52 ± 4	55 ± 5	58 ± 5	61 ± 3	60 ± 5	63 ± 4
200	47 ± 5	50 ± 2	55 ± 3	58 ± 2	57 ± 3	60 ± 2
500	43 ± 4	47 ± 3	48 ± 4	52 ± 3	51 ± 4	55 ± 3
1000	37 ± 6	40 ± 2	42 ± 2	48 ± 4	48 ± 5	54 ± 2
	BQ-4		BQ-5		BQ-6	
100	57 ± 5	60 ± 4	50 ± 5	53 ± 5	55 ± 5	58 ± 4
200	54 ± 3	58 ± 2	45 ± 3	48 ± 2	49 ± 2	52 ± 3
500	51 ± 2	55 ± 3	41 ± 2	45 ± 3	45 ± 5	50 ± 3
1000	48 ± 4	52 ± 2	35 ± 4	37 ± 2	40 ± 2	45 ± 4
	BQ-7		BQ-8		Albendazole	
100	48 ± 4	51 ± 4	51 ± 4	54 ± 2	55 ± 6	58 ± 4
200	43 ± 5	46 ± 4	46 ± 2	49 ± 4	50 ± 3	53 ± 3
500	39 ± 3	42 ± 2	42 ± 3	45 ± 2	46 ± 2	49 ± 2
1000	33 ± 2	35 ± 3	37 ± 2	40 ± 3	40 ± 4	44 ± 3

Enterococcus faecium, the zones of inhibition were measured at 6, 8, 10, 12 and 8, 10, 12 and 14 mm, respectively, when exposed to penicillin G at the concentrations of 5, 10, 15 and 20 µg/mL, respectively. Similarly, for Gram-negative bacteria like *Pseudomonas aeruginosa* and *Klebsiella pneumoniae*, the zones of inhibition were recorded at 9, 11, 12, 14 and 6, 8, 10 and 12 mm, respectively, under the influence of chloramphenicol concentrations of 5, 10, 15 and 20 µg/mL, respectively. A comparison between the antibacterial activity of the synthesized bromoquinazolinones and standard drugs is depicted in Fig. 3.

With the exception of compounds **BQ 2, 3** and **4**, all the synthesized bromoquinazolinones demonstrated significant antibacterial activity against Gram-positive bacteria. This outcome highlights the importance of introducing arylamido, aniline or N,N-dimethyl guanidinyl groups on nitrogen at the 3-position of quinazolinones to enhance their efficacy against Gram-positive bacteria. The overall antibacterial activity of the synthesized quinazolinones against Gram-negative bacteria was observed to be relatively restrained.

Conclusion

A new series of bromoquinazolinones (**BQ1-8**) has been successfully synthesized and characterized. The majority of the synthesized compounds displayed promising anthelmintic

and antibacterial activity. Among this series, **BQ 7, 8, 5, 6** and **1** exhibited the highest potency, respectively. Structural activity relationship studies suggest that incorporating arylamido, aniline or dimethyl guanidinyl groups at the nitrogen in the 3rd position and introducing electronegative bromine at the 6th position of the quinazolinone ring could enhance both anthelmintic and antibacterial activity. Further exploration involving analogs with diverse electron-modulating groups on the quinazolinone nucleus and phenyl or aryl substituents holds the potential for yielding even more potent agents. However, the synthesized quinazolinones demonstrated the modest activity against Gram-negative bacteria. Therefore, it is essential to undertake additional synthetic efforts targeting derivatives with ionizable potential, as this might effectively enhance their efficacy against Gram-negative bacteria.

ACKNOWLEDGEMENTS

The authors express their gratitude for the material support received from Sri Padmavathi School of Pharmacy, Dr. M.G.R. Educational and Research Institute and SVU College of Pharmaceutical Sciences. Additionally, the authors extend their appreciation to the authorities of PASS, Molinspiration, Osiris and Swiss ADME for generously providing free software.

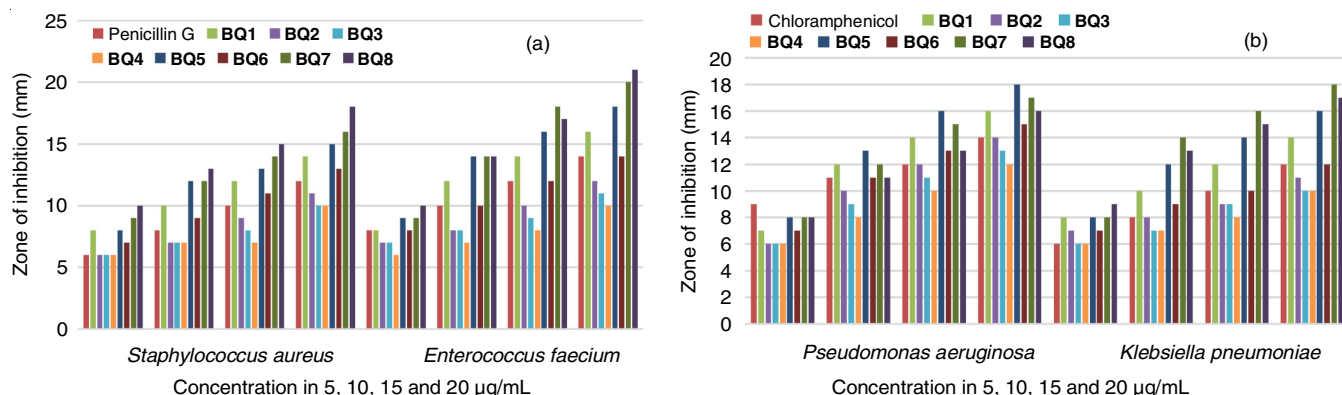


Fig. 3. Antibacterial activity of 6-bromo-2-phenyl-3-substituted quinazolin-4(3H)-ones (**BQ 1-8**) against (a) Gram-positive and (b) Gram-negative bacteria

CONFLICT OF INTEREST

The authors declare that there is no conflict of interests regarding the publication of this article.

REFERENCES

1. A. Loukas, R.M. Maizels and P.J. Hotez, *Int. J. Parasitol.*, **51**, 1243 (2021); <https://doi.org/10.1016/j.ijpara.2021.11.001>
2. N. Safi, S. Warusavithana, S.A.S. Alawi, H. Atta, A. Montresor and A. Francesco-Gabrielli, *Acta Trop.*, **197**, 105035 (2019); <https://doi.org/10.1016/j.actatropica.2019.05.026>
3. https://apps.who.int/neglected_diseases/ntddata/sth/sth.html
4. A.F. Veessenmeyer, *Pediatr. Clin. North Am.*, **69**, 129 (2022); <https://doi.org/10.1016/j.pcl.2021.08.005>
6. Global Report on Neglected Tropical Diseases (2023); <https://www.who.int/teams/control-of-neglected-tropical-diseases/global-report-on-neglected-tropical-diseases-2023>
7. H.M.P.D. Herath, A.C. Taki, B.E. Sleebbs, A. Hofmann, N. Nguyen, S. Preston, R.A. Davis, A. Jabbar and R.B. Gasser, *Adv. Parasitol.*, **111**, 203 (2021); <https://doi.org/10.1016/bs.apar.2020.10.002>
8. Y. Jiao, S. Preston, A. Hofmann, A. Taki, J. Baell, B.C.H. Chang, A. Jabbar and R.B. Gasser, *Adv. Parasitol.*, **108**, 1 (2020); <https://doi.org/10.1016/bs.apar.2019.12.003>
9. R. Karan, P. Agarwal, M. Sinha and N. Mahato, *Chem. Eng.*, **5**, 73 (2021); <https://doi.org/10.3390/chemengineering5040073>
10. S. Debnath and S.Y. Manjunath, *Int. J. Pharm. Sci. Nanotech.*, **4**, 1408 (2011); <https://doi.org/10.37285/ijpsn.2011.4.2.6>
11. M.F. Zayed, H.E.A. Ahmed, S. Ihmaid, A.-S.M. Omar and A.S. Abdelrahim, *J. Taibah Univ. Medical Sci.*, **10**, 333 (2015); <https://doi.org/10.1016/j.jtumed.2015.02.007>
12. J.N. Akester, P. Njaria, A. Nchinda, C. Le Manach, A. Myrick, V. Singh, N. Lawrence, M. Njoroge, D. Taylor, A. Moosa, A.J. Smith, E.J. Brooks, A.J. Lenaerts, G.T. Robertson, T.R. Ioerger, R. Mueller and K. Chibale, *ACS Infect. Dis.*, **6**, 1951 (2020); <https://doi.org/10.1021/acsinfecdis.0c00252>
13. A.K. Khan, *Al-Mustansiriyah J. Sci.*, **28**, 122 (2018); <https://doi.org/10.23851/mjs.v28i3.180>
14. R. Khalil and S. H. Abdulrahman, *Turkish Comput. Theor. Chem.*, **6**, 1 (2022); <https://doi.org/10.33435/tcandtc.894168>
15. E. Jafari, M.R. Khajouei, F. Hassanzadeh, G.H. Hakimelahi and G.A. Khodarahmi, *Res. Pharm. Sci.*, **11**, 1 (2016).
16. N. Nagaladinne, A.A. Hindustan and D. Nayakanti, *Asian J. Chem.*, **32**, 3067 (2020); <https://doi.org/10.14233/ajchem.2020.22930>
17. R.K. Kumarachari, S. Peta, A.S. Surur and Y.T. Mekonnen, *J. Pharm. Bioallied Sci.*, **8**, 181 (2016); <https://doi.org/10.4103/0975-7406.171678>
18. R.K. Kumarachari, M. Guruvareddy, M. Phebe, P.L. Reddy, M.S. Nithin, D. Lakshmipathi and M. Manasa, *Asian J. Chem.*, **35**, 617 (2023); <https://doi.org/10.14233/ajchem.2023.27482>
19. H.E. Hashem, *Synthesis of Quinazoline and Quinazolinone Derivatives*. IntechOpen (2020); <https://doi.org/10.5772/intechopen.89180>
20. G. Khodarahmi, E. Jafari, G. Hakimelahi, D. Abedi, M. Rahmani Khajouei and F. Hassanzadeh, *Iran. J. Pharm. Res.*, **11**, 789 (2012).
21. D.A. Filimonov, A.A. Lagunin, T.A. Glorizova, D.S. Druzhilovskii, A.V. Rudik, P.V. Pogodin and V.V. Poroikov, *Chem. Heterocycl. Compd.*, **50**, 444 (2014); <https://doi.org/10.1007/s10593-014-1496-1>
22. A. Ayar, M. Aksahin, S. Mesci, B. Yazgan, M. Gül and T. Yildirim, *Curr. Computeraided Drug Des.*, **18**, 52 (2022); <https://doi.org/10.2174/1573409917666210223105722>
23. T. Sander, Actelion's Property Explorer, Allschwil, Switzerland: Actelion's Pharmaceuticals Ltd. (2001).
24. A. Daina, O. Michielin and V. Zoete, *Sci. Rep.*, **7**, 42717 (2017); <https://doi.org/10.1038/srep42717>
25. S.S. Chitikina, P. Buddiga, R.P. Mailavaram, K.N. Venugopala, P.K. Deb, A.B. Nair, B. Al-Jaidi and S. Kar, *Med. Chem. Res.*, **29**, 1600 (2020); <https://doi.org/10.1007/s00044-020-02586-5>
26. B. Jin, J.Y. Chen, Z.L. Sheng, M.Q. Sun and H.L. Yang, *Molecules*, **27**, 1103 (2022); <https://doi.org/10.3390/molecules27031103>
27. B. Aneja, M. Azam, S. Alam, A. Perwez, R. Maguire, U. Yadava, K. Kavanagh, C.G. Daniliuc, M.M.A. Rizvi, Q.M.R. Haq and M. Abid, *ACS Omega*, **3**, 6912 (2018); <https://doi.org/10.1021/acsomega.8b00582>
28. CLSI, M100 Performance Standards for Antimicrobial Susceptibility Testing, 29th ed. CLSI; Wayne, PA, USA (2019).